Supporting Information

Ultrathin PtCu hexapod nanocrystals with enhanced catalytic performance for electro-oxidation reactions

Kai Wang,[a] Rinrada Sriphathoorat,[a] Shuiping Luo,[a] Min Tang,[a] Hongyu Du[a] and Pei Kang Shen*[ab]

[a] *State Key Laboratory of Optoelectronic Materials and Technologies, School of Materials Science and Engineering, Sun Yat-sen University, Guangzhou, 510275, P. R. China.*

[b] *Collaborative Innovation Center of Sustainable Energy Materials, Guangxi University, Nanning 530004, China. E-mail: pkshen@gxu.edu.cn*

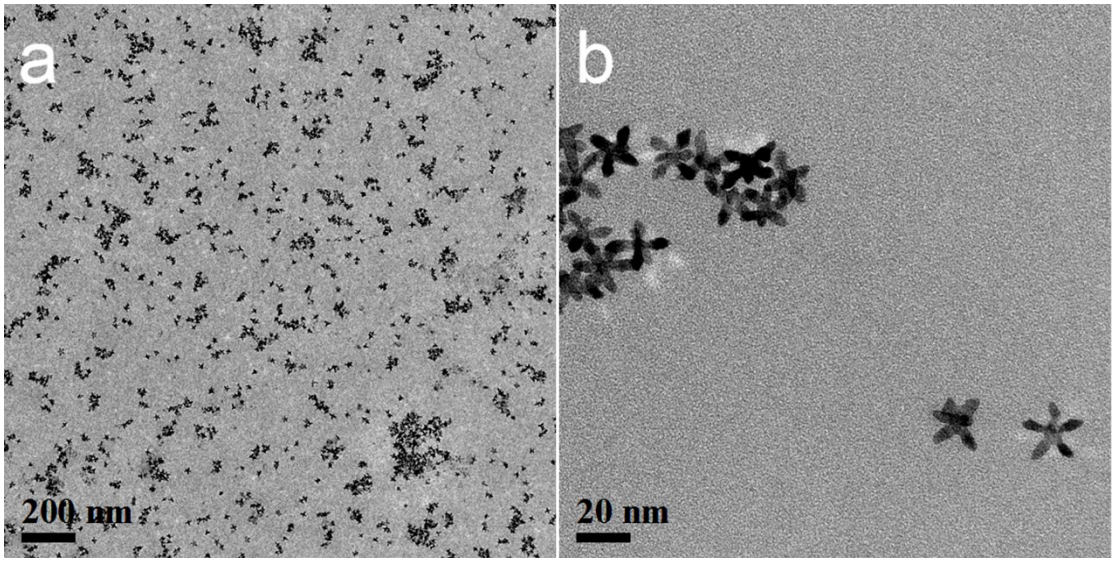

Figure S1. Additional (a) low-magnification TEM and (b) high-magnification TEM images of as-prepared ultrathin PtCu hexapod nanocrystals.

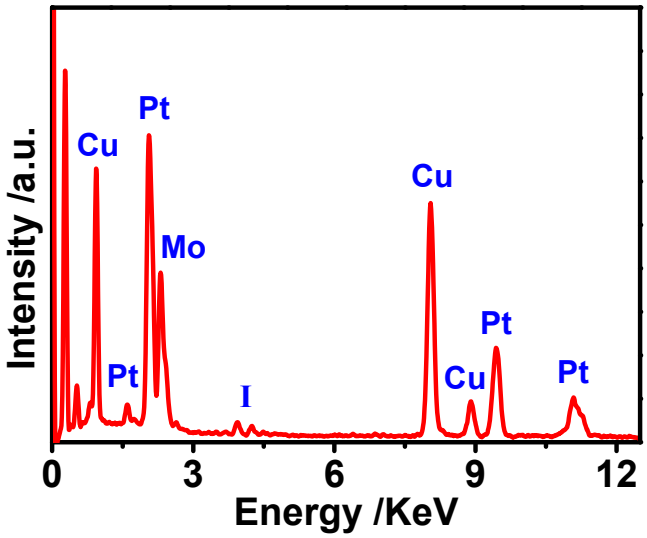

Figure S2. TEM-EDS spectrum of the prepared ultrathin PtCu hexapod nanocrystals

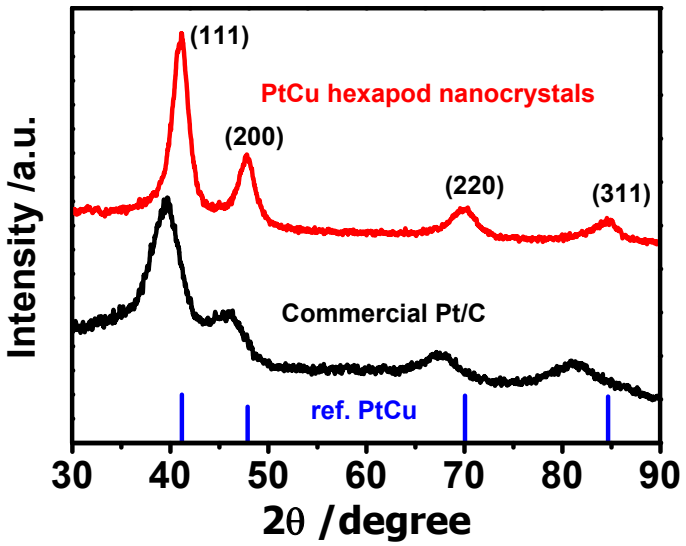

Figure S3. X-ray diffraction (XRD) patterns of ultrathin PtCu hexapod nanocrystals and commercial Pt/C. The standard diffraction peaks of PtCu alloy compound is also shown for comparison.

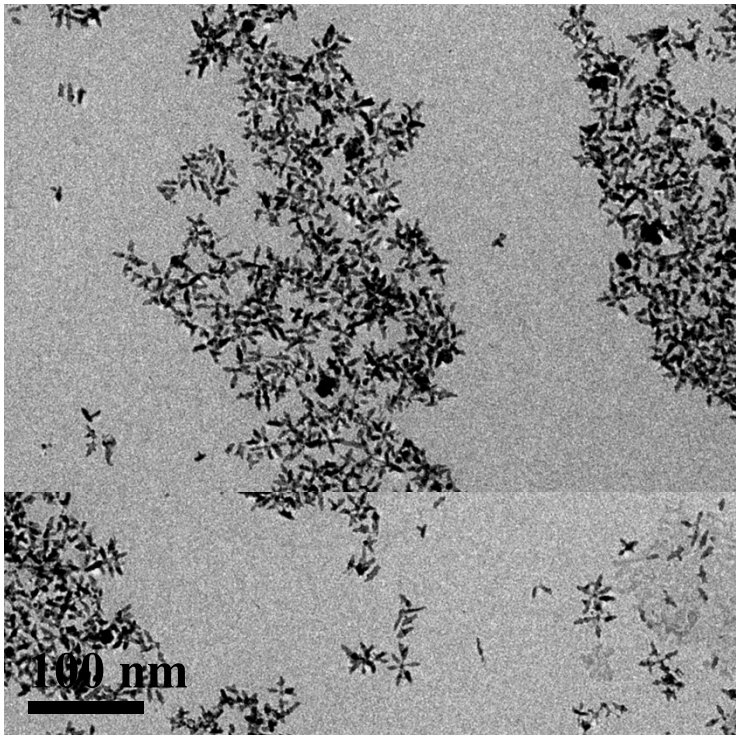

Figure S4. Large-area TEM image of nanocrystals prepared by using the standard procedure but with 30.0 mg mL^{-1} NaI.

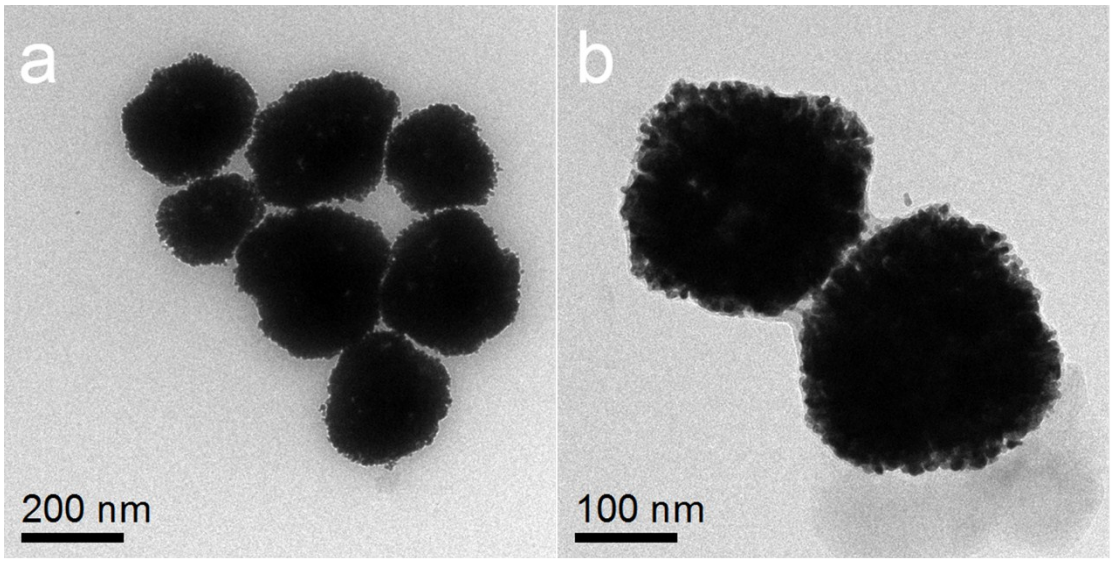

Figure S5. Typical TEM images of the nanocrystals prepared by using the standard procedure but in the absence of Cu precursor ($Cu(NO_3)_2 \cdot 3H_2O$).

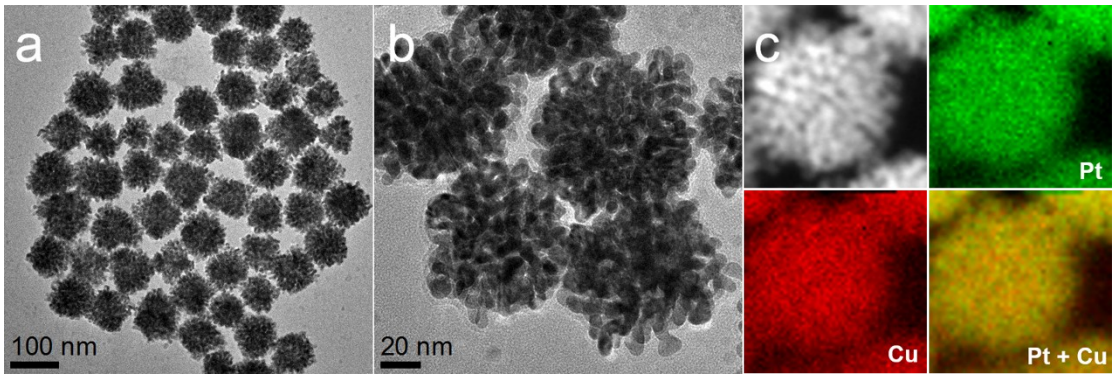

Figure S6. (a and b) Typical TEM images of the nanocrystals prepared with feeding molar ratio of Pt/Cu = 3/1. (c) HAADF-STEM image and elemental mapping images of a single PtCu nanodendrites.

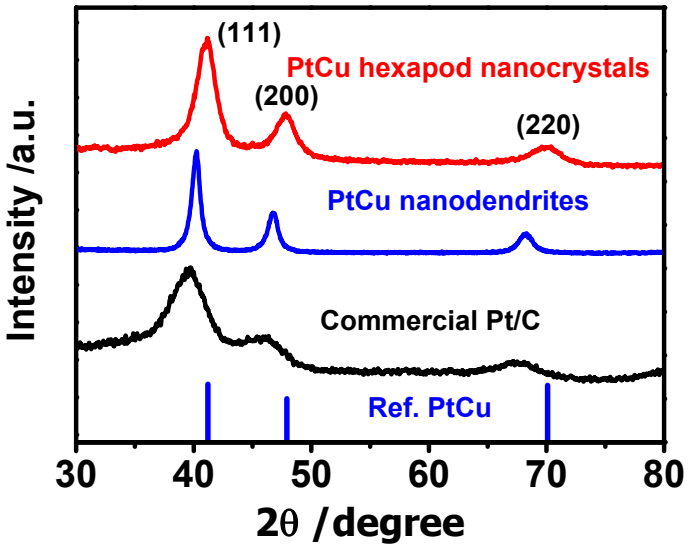

Figure S7. XRD patterns of PtCu nanodendrites, ultrathin PtCu hexapod nanocrystals and commercial Pt/C. The standard diffraction peaks of PtCu alloy compound is also shown for comparison.

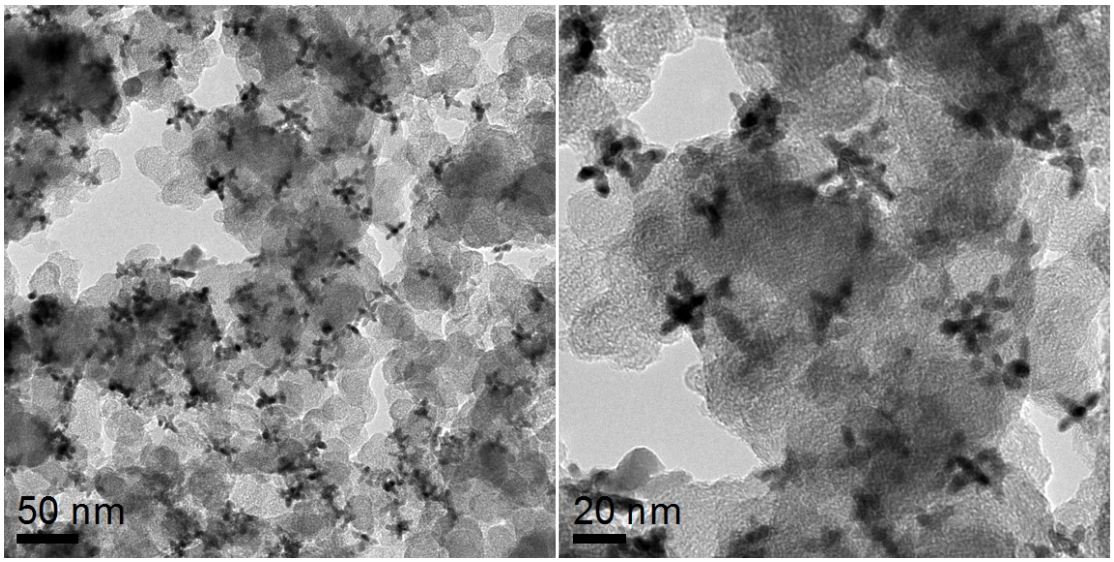

Figure S8. Typical TEM images of ultrathin PtCu hexapod nanocrystals loaded on carbon.

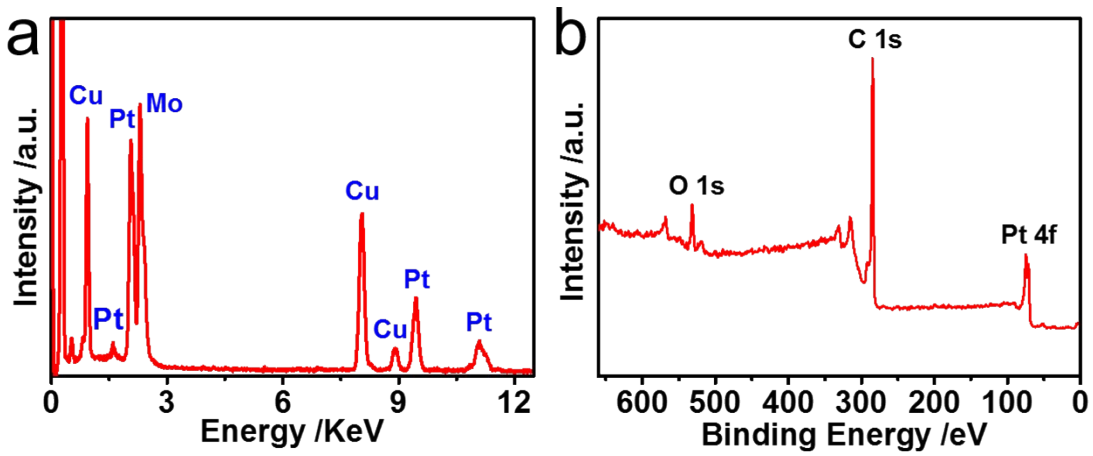

Figure S9. (a) TEM-EDS spectrum and (b) raw XPS intensity data of carbon-supported ultrathin PtCu hexapod nanocrystals. Two I 3d peaks should be located at 71.5 and 74.8 eV, respectively *(J. Am. Chem. Soc.* 95, 751, 1973).

Table S1. The catalytic activities of different catalysts for methanol oxidation reaction. All these electrochemical measurements were carried out in 0.5 M H_2SO_4 + 1 M CH_3OH solution at a sweep rate of 50 mV s^{-1}.

Catalysts		**Mass activity ($A\ mg_{Pt}^{-1}$)**	**Specific activity ($mA\ cm^{-2}$)**	**Ref.**
Pt-based nanodendrites	Pt-on-Pd nanodendrites	0.49		1
	PtRuFe nanodendrites	1.14	2.03	2
	PtPd nanodendrites	0.41		3
	PtFe@Pt nanodendrites	0.82		4
PtCu nanoalloy	Hollow-PtCu/C	0.89	1.77	5
	Nanoporous $Pt_{60}Cu_{40}$	0.75	4.90	6
	PtCu nanoframes		1.97	7
	PtCu hollow nanocrystals		2.08	8
	$PtCu_2$ nanowire networks	1.29	1.87	9
	Ultrathin PtCu hexapods	2.01	3.54	This work
	PtCu nanodendrites	0.39	1.99	This work

Table S2. The sizes and MOR activities of Pt/Cu hexapod concave nanocrystals (Ref. 17 in text), corroded $PtNi_3$ (Ref. 32 in text), and ultrathin PtCu hexapod nanocrystals.

Catalysts	Size of the whole nanocrystals (nm)	Length of pods (nm)	Diameter of pods (nm)	Aspect ratio of pods	MOR activity (A mg_{Pt}^{-1})	Ref.
Pt/Cu hexapod concave nanocrystals	About 18	About 5.25	About 5.33	1.0	About 1.15	Ref. 17 in text
Corroded $PtNi_3$	About 11.3	About 2.48	About 2.73	0.9		Ref. 32 in text
Ultrathin PtCu hexapods	20.0	10.2	3.57	2.9	2.01	This work

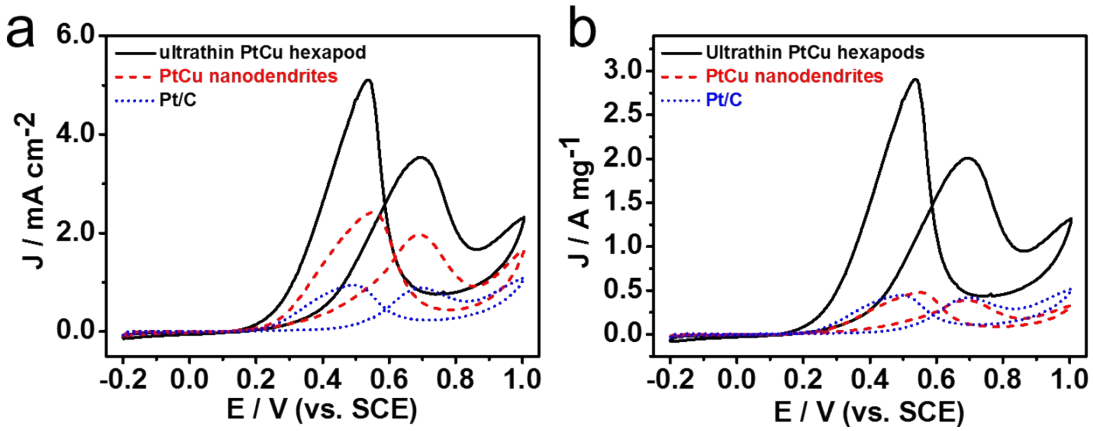

Figure S10. (a) Specific activities and (b) mass activities of the as-prepared ultrathin PtCu hexapod nanocrystals, PtCu nanodendrites and commercial Pt/C in 0.5 M H_2SO_4 + 1 M CH_3CH_2OH solution. Sweep rate: 50 mV s^{-1}. Specific and mass activities were normalized to the ECSAs and loading amount of Pt, respectively.

For specific activities, the peak value of ultrathin PtCu hexapods in the forward potential scan is 1.8 and 4.0 times higher than those of PtCu nanodendrites and commercial Pt/C, respectively. For mass activities, the peak value of ultrathin PtCu hexapods is 5.2 and 4.8 times higher than those of PtCu nanodendrites and commercial Pt/C, respectively.

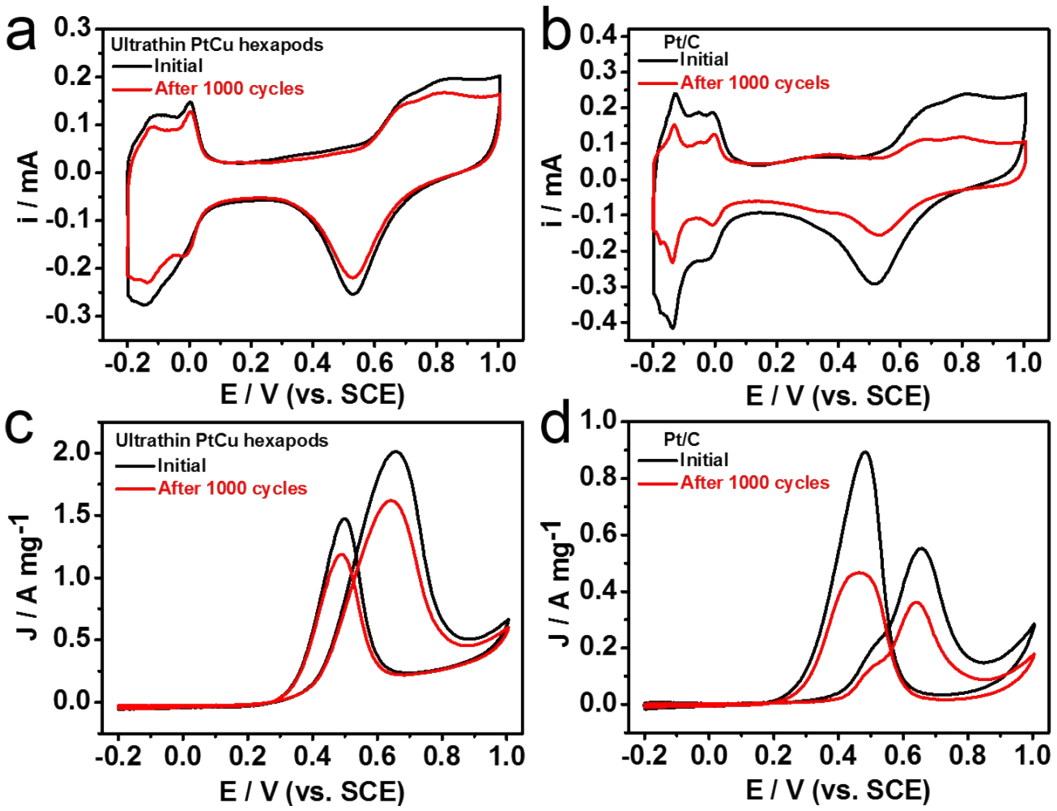

Figure S11. Electrocatalytic stability tests of the as-prepared ultrathin PtCu hexapod nanocrystals and commercial Pt/C. CV profiles of (a) the ultrathin PtCu hexapod nanocrystals and (b) commercial Pt/C in 0.5 M H_2SO_4 solution before and after stability tests. Mass activities of (c) the ultrathin PtCu hexapod nanocrystals and (d) commercial Pt/C in 0.5 M H_2SO_4 + 1 M CH_3OH solution before and after stability tests. The tests were carried out in 0.5 M H_2SO_4 + 1 M CH_3OH solution with the cyclic potential between -0.2 and 1.0 V for 1,000 cycles at a sweep rate of 50 mV s^{-1}.

After 1,000 cycles, the ECSAs was reduced by 24.7 % for the as-prepared ultrathin PtCu hexapod nanocrystals and 58.0 % for Pt/C, and the mass activities were reduced by 19.4 % for the as-prepared ultrathin PtCu hexapod nanocrystals and 34.5 % for Pt/C.

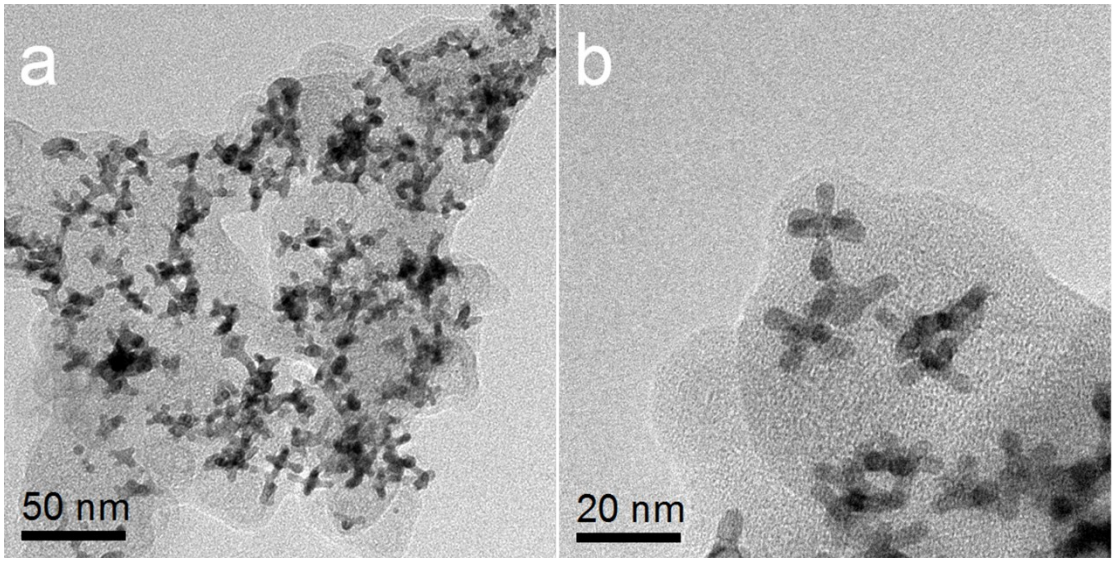

Figure S12. Typical TEM images of ultrathin PtCu hexapod nanocrystals after the durability tests.

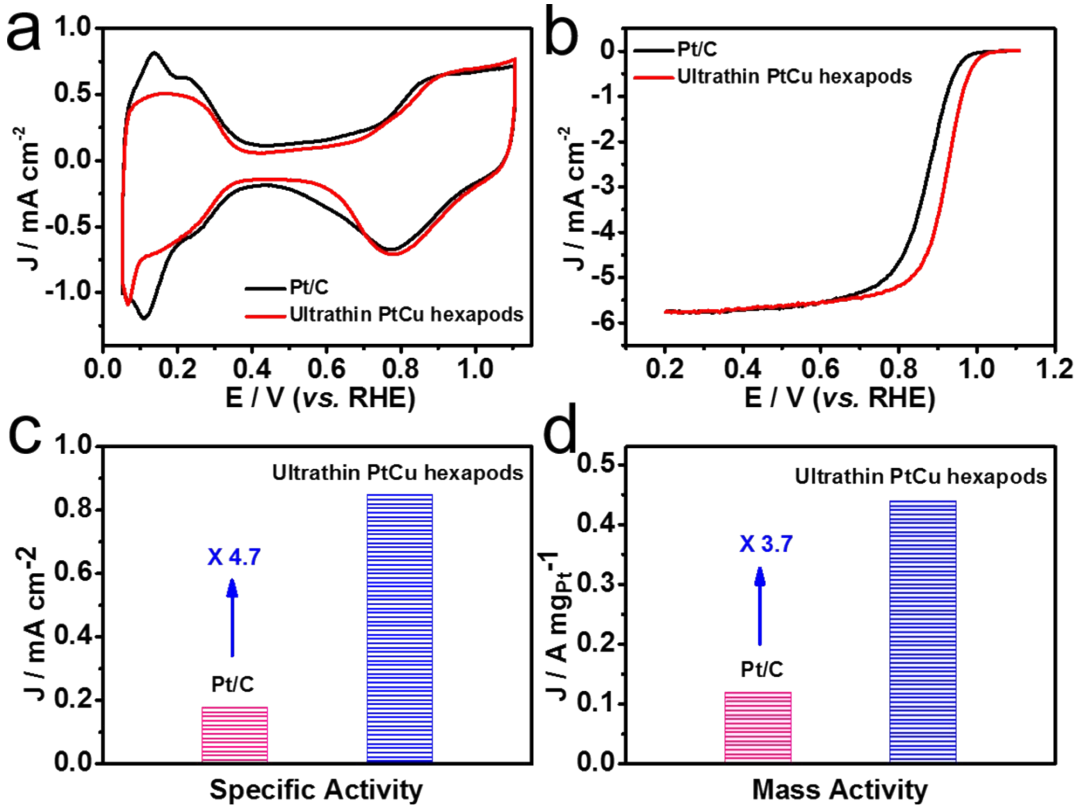

Figure S13. Electrocatalytic properties of ultrathin PtCu hexapod nanocrystals and commercial Pt/C catalysts for ORR. (a) CV curves recorded at room temperature in a N_2-saturated 0.1 M $HClO_4$ solution with a sweep rate of 50 mV s^{-1}. (b) ORR polarization curves recorded at room temperature in an O_2-saturated 0.1 M $HClO_4$ solution with a sweep rate of 5 mV s^{-1} and a rotation rate of 1,600 rpm. (c, d) Specific activity and mass activity at 0.9 V *vs.* RHE of these two catalysts, which were normalized to the ECSA and the loading amount of Pt, respectively. In (a) and (b), current densities were normalized to the geometric area of the rotating disk electrode (0.196 cm^2). The Pt loadings were 4.7 and 4.5 μg for ultrathin PtCu hexapod nanocrystals and commercial Pt/C in ORR tests.

Figure S13a compares the CV curves of ultrathin PtCu hexapod nanocrystals and commercial Pt/C catalysts. The ECSAs, which were calculated by integrating the charges on the hydrogen adsorption region (0.05-0.40 V), were 45.0 $m^2g^{-1}_{Pt}$ for ultrathin PtCu hexapods, and 58.1 $m^2g^{-1}_{Pt}$ for Pt/C. **Figure S13b** shows the ORR polarization curves for ultrathin PtCu hexapods and commercial Pt/C catalysts. The half-wave potentials of ultrathin PtCu hexapods and Pt/C are 0.919 and 0.871 V, respectively, indicating that the catalytic activity of ultrathin PtCu hexapod nanocrystals is higher than that of Pt/C. As shown in **Figure S13c** and **S13d**, the specific and mass activities of the ultrathin PtCu hexapods are 4.7 and 3.7 times greater than those of Pt/C catalysts.

Reference

1. L. Wang, Y. Nemoto and Y. Yamauchi, *J. Am. Chem. Soc.*, 2011, **133**, 9674-9677.
2. Z. Cai, Y. Kuang, X. Qi, P. Wang, Y. Zhang, Z. Zhang and X. Sun, *J. Mater. Chem. A.*, 2015, **3**, 1182-1187.
3. L. Wang and Y. Yamauchi, *J. Am. Chem. Soc.*, 2013, **135**, 16762-16765.
4. J. Zhu, M. Xiao, K. Li, C. Liu and W. Xing, *Chemical communications*, 2015, **51**, 3215-3218.
5. X. Huang, Y. Chen, E. Zhu, Y. Xu, X. Duan and Y. Huang, *J. Mater. Chem. A.*, 2013, **1**, 14449-14454.
6. H.-J. Qiu, X. Shen, J. Wang, A. Hirata, T. Fujita, Y. Wang and M. Chen, *ACS Catalysis*, 2015, **5**, 3779-3785.
7. X. Yu, L. Li, Y. Su, W. Jia, L. Dong, D. Wang, J. Zhao and Y. Li, *Chemistry–A European Journal*, 2016, **22**, 4960-4965.
8. X. Yu, D. Wang, Q. Peng and Y. Li, *Chemical communications*, 2011, **47**, 8094-8096.
9. M. Xiao, S. Li, X. Zhao, J. Zhu, M. Yin, C. Liu and W. Xing, *ChemCatChem*, 2014, **6**, 2825-2831.